Quenching of Tryptophan Fluorescence by the Active-Site Disulfide Bridge in the DsbA Protein from *Escherichia coli*†

Jens Hennecke,‡ Alain Sillen,§ Martina Huber-Wunderlich,‡ Yves Engelborghs,§ and Rudi Glockshuber*,‡

Institut für Molekularbiologie und Biophysik, Eidgenössische Technische Hochschule Hönggerberg, CH-8093 Zürich, Switzerland, and Laboratory of Chemical and Biological Dynamics, University of Leuven, Celestijnenlaan 200 D, B-3001 Leuven, Belgium

Received December 9, 1996; Revised Manuscript Received March 3, 1997⊗

ABSTRACT: The disulfide oxidoreductase DsbA is a strong oxidant of protein thiols and required for efficient disulfide bond formation in the bacterial periplasm. The enzyme consists of a thioredoxin-like domain and a second, α-helical domain which is inserted into the thioredoxin motif. Reduction of the active-site disulfide in the thioredoxin domain causes a more than 3-fold increase in tryptophan fluorescence. However, both tryptophan residues of the protein, W76 and W126, are not in contact with the disulfide and located in the α-helical domain. Analysis of the variants W76F and W126F revealed that the fluorescence of W126 is fully quenched in every redox state of DsbA. W126 is also a sink for nonradiative energy transfer from W76. In oxidized DsbA, W76 is quenched by an intramolecular, dynamic quenching process which involves energy transfer from W76 via F26 to the disulfide. The contributions of the disulfide bridge and the tryptophan residues to the near-UV CD spectra were also quantified. Analysis of the thermodynamic stabilities of the variants W76F and F26L revealed that the interdomain contact between W76 and F26 strongly contributes to the overall stability of DsbA, and selectively stabilizes its oxidized form. The DsbA variant F26L is the most oxidizing disulfide oxidoreductase known so far.

Enzymes of the thiol−disulfide oxidoreductase (TDOR)[1] family are involved in numerous processes in prokaryotic and eukaryotic cells, including protein folding, DNA synthesis, cytochrome biogenesis, and photosynthesis [for reviews, see Gilbert (1990), Bardwell and Beckwith (1993), and Loferer and Hennecke (1994)]. All TDORs catalyze the formation or reduction of structural, regulatory, or catalytic disulfide bridges in target proteins by disulfide exchange reactions with their substrates.

The C-X-X-C motif of the active-site disulfide is characteristic for all TDORs. Reduction of the catalytic disulfide bridge in thioredoxin, DsbA, and TlpA has been shown to cause a strong increase in tryptophan fluorescence (Holmgren, 1972; Wunderlich & Glockshuber, 1993; Loferer *et al.*, 1995). Common to *Escherichia coli* thioredoxin and TlpA from *Bradyrhizobium japonicum* (Loferer *et al.*, 1993) are two tryptophan residues that are located in the −1 (proximal tryptophan) and −4 (distal tryptophan) positions with respect to the first active-site cysteine. For thioredoxin, it was demonstrated that the distal tryptophan is mainly responsible for the fluorescence increase (Krause & Holmgren, 1991; Slaby *et al.*, 1996). The proximal tryptophan is conserved among all known thioredoxins and thioredoxin domains of eukaryotic protein disulfide isomerase (PDI).

In this study, we undertook a detailed analysis of the fluorescence properties of DsbA from *Escherichia coli*. DsbA is a monomeric, periplasmic 21.1 kDa protein (189 aa) and required for efficient disulfide bond formation (Bardwell *et al.*, 1991; Kamitani *et al.*, 1992). The enzyme contains a single, catalytic disulfide with the active-site sequence C^{30}-P^{31}-H^{32}-C^{33}.

Recent work has shown that DsbA is the most oxidizing member of the TDOR family and donates its disulfide bond extremely rapidly to folding proteins (Wunderlich *et al.*, 1993a; Zapun *et al.*, 1993; Zapun & Creighton, 1994; Darby & Creighton, 1995). *In vivo*, DsbA is recycled as an oxidant by disulfide exchange with DsbB, a protein from the inner membrane of *E. coli* (Bardwell *et al.*, 1993; Jander *et al.*, 1994; Kishigami *et al.*, 1995; Guilhot *et al.*, 1995).

The three-dimensional X-ray structure of oxidized DsbA (Martin *et al.*, 1993) has revealed that the enzyme possesses a thioredoxin-like domain (residues 1−62 and 139−189), a motif found in all known structures of disulfide oxidoreductases (Martin, 1995). The sequence of the thioredoxin-like domain of DsbA is, however, only 10% identical with *E. coli* thioredoxin. DsbA possesses a second domain (residues 63−138) of unknown function, which is inserted into the thioredoxin motif and exclusively consists of α-helices (Figure 1). In contrast to thioredoxin, DsbA does not contain tryptophans amino-terminal to its catalytic disulfide. Nevertheless, a strong, about 3-fold increase in tryptophan fluorescence is observed upon reduction of its disulfide (Wunderlich & Glockshuber, 1993; Zapun *et al.*, 1993) which

† This project was supported by a research grant from the ETH Zürich (Switzerland) and by the National Fund for Scientific Research G.0242.96 (Belgium).

* To whom correspondence should be addressed. Phone: ++41-1-633-6819. Fax: ++41-1-633-1036. E-mail: RUDI@MOL.BIOL.ETHZ.CH.

‡ Eidgenössische Technische Hochschule Hönggerberg.

§ University of Leuven.

⊗ Abstract published in *Advance ACS Abstracts,* May 1, 1997.

[1] Abbreviations: CD, circular dichroism; DTNB, 5,5′-dithiobis(2-nitrobenzoic acid); DTT, 1,4-dithio-DL-threitol; EDTA, ethylenediaminetetraacetic acid; GdmCl, guanidinium chloride; GSH, reduced glutathione; GSSG, oxidized glutathione; IPTG, isopropyl β-D-thiogalactoside; MOPS, 3-(*N*-morpholino)propanesulfonic acid; SDS, sodium dodecyl sulfate; TDOR, thiol−disulfide oxidoreductase; Tris, 2-amino-2-(hydroxymethyl)-1,3-propanediol; UV, ultraviolet; X-Gal, 5-bromo-4-chloro-3-β-D galactopyranoside.

S0006-2960(96)03017-6 CCC: $14.00 © 1997 American Chemical Society

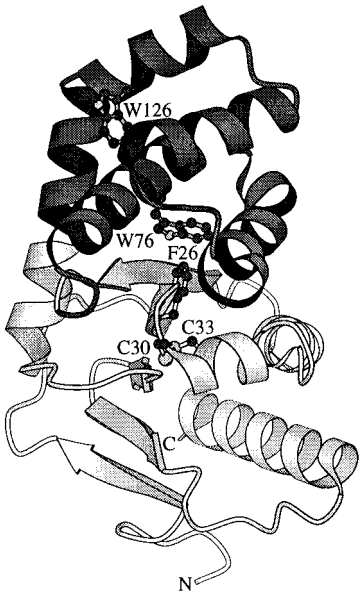

FIGURE 1: Molscript diagram (Kraulis, 1991) of the X-ray structure of oxidized DsbA from *E. coli* (Martin *et al.*, 1993). The thioredoxin-like domain and the α-helical domain of DsbA are indicated in white and black, respectively. The cysteine side chains, the two single tryptophan residues, and the side chain of F26 are also shown.

was used to measure the redox potential of the protein and to monitor its interaction with substrate proteins (Wunderlich & Glockshuber, 1993; Zapun *et al.*, 1993; Wunderlich *et al.*, 1993a; Grauschopf *et al.*, 1995). Interestingly, both tryptophans of DsbA, W76 and W126, are not contained in the thioredoxin domain and are located in the α-helical domain (Figure 1). W76 is buried and about 12 Å apart from the disulfide, whereas W126 is even further away from the disulfide bridge (about 20 Å) and partially solvent-accessible. Hence, quenching of the tryptophan fluorescence by the direct contact between W76 and the disulfide is not possible. In this study, we have constructed DsbA variants where the tryptophan residues were replaced by phenylalanine residues. The variants were characterized with respect to *in vivo* function, biochemical properties, and the origin of the fluorescence quenching. In addition, the involvement of F26 in the quenching process was investigated. F26 is located exactly between the disulfide bridge and the buried W76 at the domain interface.

EXPERIMENTAL PROCEDURES

Materials. 1,4-Dithio-DL-threitol (DTT), reduced glutathione (GSH), oxidized glutathione (GSSG), sodium succinate, amino acids, ampicillin, dithionitrobenzoic acid (DTNB), 5-bromo-4-chloro-3-β-D-galactopyranoside (X-Gal), and polymyxin B sulfate were purchased from Sigma (Buchs, Switzerland). Maltose was from ICN (Ohio), isopropyl β-D-thiogalactoside (IPTG) was from AGS GmbH (Heidelberg, Germany), DE52- and CM52-cellulose were purchased from Whatman (Maidstone, United Kingdom), and phenyl-Sepharose was obtained from Pharmacia (Uppsala, Sweden). All other chemicals were from Merck (Darmstadt, Germany), Fluka (Buchs, Switzerland), or Jansen Chemica (Geel, Belgium) and of the highest purity available.

Solutions were filtered (0.22 μm), degassed, and assayed for spectral purity.

Mutagenesis. For construction and expression of the *dsbA* mutants, the phasmid pDsbA2 was used, harboring the *dsbA* gene under control of the *trc*-promotor (Hennecke *et al.*, 1997). Site-directed mutagenesis was performed according to Kunkel *et al.* (1985, 1987) using the helper phage M13KO7 (Vieira & Messing, 1987) and the kit supplied by Bio-Rad (Hercules, CA). The following oligonucleotides were used:

F26L: 5′-GTG CGG GCA GAA GAA GCT TAA AAA CTC CAG CAC TTG-3′

W76F: 5′-CGC CAT CGC CAC AGC GAA AGC TTG AGT CAG ATC TTT G-3′

W126F: 5′-GAT TTC ACC ACA AAG CTG TTA AAC GCT GCA TCA TAC TCT TCA CCT TTA A-3′

Mutants were identified by restriction analysis and verified by sequencing the whole mutated genes using the T7 sequencing kit (Pharmacia, Uppsala, Sweden).

Expression and Purification of DsbA. Cells of the DsbA-deficient strain *E. coli* THZ2 (*dsbA::kan, recA::cam,* λmalF-lacZ102; with respect to this genotype, THZ2 is isogenic to THZ7; Grauschopf *et al.*, 1995) harboring the respective expression plasmids were used for overproduction of the DsbA variants. Growth of bacterial cultures and purification of the proteins from the periplasm of *E. coli* by anion exchange chromatography on DE52, hydrophobic chromatography on phenyl-Sepharose, and cation exchange chromatography on CM 52 were performed as described (Wunderlich & Glockshuber, 1993; Hennecke *et al.*, 1997). All DsbA preparations were ≥99% pure as judged by Coomassie-stained SDS gels. The molecular mass of each variant was confirmed by electrospray mass spectrometry (error ≤1 Da). Molar extinction coefficients were determined according to Gill and von Hippel (1989). All DsbA variants were obtained in the oxidized form, as shown by the lack of thiol groups (Ellman, 1959). Proteins were dialyzed against distilled water and stored at −20 °C.

Determination of DsbA Activity in Vivo. The *dsbA* mutants were tested for their ability to complement the phenotypes of *E. coli dsbA*$^-$ strains, namely, the lack of motility (Dailey & Berg, 1993) and the ability to express functional β-galactosidase in the periplasm (Bardwell *et al.*, 1991). For all assays, *E. coli* THZ2 (Grauschopf *et al.*, 1995) was used. Motility assays were performed at 37 °C on 0.3% agar plates containing ampicillin (100 mg/L) and either rich medium (2×YT) or minimal medium supplemented with all amino acids except cysteine and cystine (Griffey & Redfield, 1985). β-Galactosidase activity was tested at 37 °C on indicator plates containing one of the above media, supplemented with 0.4% maltose, 0.004% X-Gal, 1.5% agar, and 100 mg/L ampicillin.

Measurement of Catalytic Activity in Vitro. The *in vitro* activities of DsbA WT and variants were tested by their ability to accelerate the reduction of GSSG (5 mM) by reduced DTT (5 mM) in 10 mM acetic acid/NaOH, pH 4.5 at 25 °C. The reaction was followed by the increase in absorbance at 287 nm (Wunderlich *et al.*, 1995).

Circular Dichroism Spectra. CD spectra were measured at 25 °C on a Jasco 710 CD spectropolarimeter, accumulated 16 times and corrected for the buffer. Far- and near-UV CD spectra were measured in 0.02 cm and 1 cm quartz cuvettes, respectively. Proteins (35 μM) were dissolved in 10 mM sodium sulfate, 1 mM sodium phosphate, pH 7.0.

Samples of reduced DsbA additionally contained 100 μM DTT. The contributions of the disulfide bridge and the tryptophan residues to the CD signal were determined with the difference spectra between the oxidized and reduced form of each variant and the difference spectra between the WT and each tryptophan variant, respectively.

Steady-State Fluorescence Measurements. Fluorescence measurements were performed at 25 °C on a HITACHI F-4000 spectrofluorometer in stirred 1.0 cm (excitation path) × 0.5 cm (emission path) quartz cuvettes. The excitation wavelength was 280 or 295 nm (5 nm bandwidth), and the emission at 300−400 nm was recorded with a bandwidth of 10 nm at a scan speed of 60 nm/min and a step size of 0.2 nm. For fluorescence measurements at a constant wavelength, the signal was recorded for 20 s and averaged. Samples contained 1 μM DsbA in 1 mL of 100 mM sodium phosphate, 1 mM EDTA, pH 7.0. Reduction and unfolding of DsbA were accomplished by incubation in 1 mM DTT and 6 M GdmCl, respectively.

Quantum yield measurements were performed on a SPEX spectrofluorometer (Fluorolog 1691) with excitation and emission slits at 7.2 and 3.6 nm, respectively. For selective observation of the tryptophan residues, an excitation wavelength of 295 nm was used. Buffer conditions were the same as in the fluorescence lifetime measurements (50 mM potassium phosphate/NaOH, pH 7.0, containing 1 mM EDTA and adjusted with potassium chloride to an ionic strength of 100 mM).

All fluorescence spectra were corrected for the buffer and the wavelength dependence of the emission monochromator and the photomultiplier.

Fluorescence Quenching by Acrylamide. The fluorescence of DsbA (10 μM in 80 mM sodium phosphate, pH 7.0, 0.8 mM EDTA) was quenched by stepwise addition of small aliquots of an 8 M acrylamide solution (in the same buffer) at 25 °C (Eftink & Ghiron, 1976). Samples of reduced DsbA additionally contained 5 mM DTT. An excitation wavelength of 295 nm and an emission wavelength of 332 nm were used. The measured fluorescence was corrected for the volume increase and the inner filter effect on the excitation beam caused by acrylamide ($\epsilon_{295} = 0.23$ M^{-1} cm^{-1}).

Fluorescence Lifetime Measurements. Fluorescence lifetimes were measured using automatic multifrequency phase fluorometry between 0.4 MHz and 1 GHz as described previously (Sillen *et al.*, 1996). *N*-Acetyltryptophanamide in 0.1 M sodium phosphate buffer at pH 7.0 with a fluorescence lifetime of 2.95 ns (Szabo, 1989) or *p*-terphenyl in cyclohexane with a lifetime of 1.04 ns (Desie *et al.*, 1986) was used as reference.

To determine whether the fluorescence quenching by the disulfide is of dynamic and/or static nature, we compared the relation between the fluorescence intensity of oxidized and reduced DsbA and the relation between the "average" lifetimes of oxidized and reduced DsbA. This "average" lifetime is defined as $\langle\tau\alpha\rangle = \sum a_i\tau_i$. The total fluorescence intensity $I_{fluo} = \sum I_{0i}\tau_i$, where I_0 is the amplitude. The amplitude fraction a_i equals $I_{0i}/\sum I_{0j}$ ($I_{0i} = a_i\sum I_{0j}$). Thus, I_{fluo} equals $(\sum a_i\tau_i)(\sum I_{0j})$.

Comparison of oxidized and reduced DsbA yields

$$(I_{fluo,ox})/(I_{fluo,red}) = (\sum a_i\tau_i)^{ox}(\sum I_{0j})^{ox}/(\sum a_i\tau_i)^{red}(\sum I_{0j})^{red} \quad (1)$$

In the case where

$$(I_{fluo,ox})/(I_{fluo,red}) = (\sum a_i\tau_i)^{ox}/(\sum a_i\tau_i)^{red} \quad (2)$$

$(\sum I_{0j})^{ox}$ and $(\sum I_{0j})^{red}$ are identical, implying no static quenching.

Quantum Yield Measurements. Quantum yields were determined relative to tryptophan in aqueous solution according to the method of Parker and Rees (1960) using a quantum yield for tryptophan in water of 0.14 (Chen, 1967).

Calculation of Energy Transfer. Energy transfer between W76 and W126 was calculated according to the theory of Förster (1948). The crystal structure of oxidized DsbA (Martin *et al.*, 1993) was used to determine the distance and the orientation factor, and the refractive index of the protein was assumed to be 1.5 (Desie *et al.*, 1986). The ^1L_b state is ignored in the calculations of the geometric orientation factor since the absorption at 295 nm and the fluorescence correspond to the ^1L_a state transition (Harris & Hudson, 1990).

The efficiency of energy transfer between W76 and W126 ($E_{(W76\rightarrow W126)}$) was also calculated from experimental rate constants according to eq 3:

$$E_{(W76\rightarrow W126)} = k_{Etr(W76\rightarrow W126)}/k \quad (3)$$

where $k_{Etr(W76\rightarrow W126)}$ is the rate constant for energy transfer from W76 to W126 and k is the rate constant for the fluorescence decay, as calculated from the lifetimes with the largest amplitude.

GdmCl-Induced Unfolding Equilibria. The free energies of stabilization of oxidized and reduced DsbA were determined on the basis of a two-state equilibrium. DsbA (1 μM) was incubated at 25 °C in degassed 100 mM sodium phosphate, pH 7.0, 1 mM EDTA containing different concentrations of GdmCl for 3 days. Reduced samples additionally contained 1 mM DTT. For refolding experiments, DsbA was first denatured in 4 M GdmCl, 100 mM sodium phosphate, pH 7.0, 1 mM EDTA for 1 h at room temperature prior to incubation at different GdmCl concentrations. The transitions were followed at the emission wavelengths with the largest signal change upon denaturation (excitation at 280 nm). Data were evaluated according to a six-parameter fit as described previously (Santoro & Bolen, 1988; Wunderlich *et al*., 1993b) and normalized.

Determination of the Redox Potential. The redox potential of the active-site disulfide was determined fluorometrically by measuring the equilibrium constant between DsbA and glutathione, assuming no significant equilibrium concentrations of DsbA/glutathione mixed disulfides (Wunderlich & Glockshuber, 1993). DsbA (1 μM) was incubated under a nitrogen atmosphere with 0.1 mM GSSG and different concentrations of GSH (0.003−3 mM) in 100 mM sodium phosphate, pH 7.0, 1 mM EDTA for 20 h at 25 °C. The fraction of reduced DsbA at equilibrium (R) was measured using the specific DsbA fluorescence at 332 nm (excitation at 280 nm). The equilibrium constant was determined according to

$$R = ([GSH]^2/[GSSG])/[K_{eq} + ([GSH]^2/[GSSG])] \quad (4)$$

The redox potential (E_0') was calculated using the Nernst equation with a value of −240 mV for the standard redox potential of glutathione (Rost & Rapoport, 1964).

Table 1: Relative Catalytic Activities,[a] Molar Extinction Coefficients,[b] and Quantum Yields[c] of DsbA WT, DsbA Variants, and *E. coli* Thioredoxin

protein	rel act. (%)	ϵ_{280} (M^{-1} cm^{-1})	quantum yield	
			oxidized	reduced
WT	100	23322	0.03	0.10
F26L	122	23919	0.06	0.09
W76F	99	17127	≤0.01	≤0.01
W126F	101	17680	0.05	0.20
W76FW126F	89	11542	≤0.01	≤0.01
thioredoxin	nd	14430	0.01	0.05

[a] Measured by catalysis of the reduction of oxidized glutathione by reduced DTT, at pH 4.5. [b] Determined according to Gill and von Hippel (1989). [c] Determined by comparison with free tryptophan ($Q = 0.14$) according to Parker and Rees (1960) (excitation at 295 nm).

RESULTS

Construction, Phenotypic Characterization, and in Vitro Activity of the DsbA Variants. Mutations in the *dsbA* gene were introduced by oligonucleotide-directed mutagenesis according to Kunkel *et al*. (1985, 1987) using the phasmid pDsbA2 (Hennecke *et al.*, 1997) and confirmed by dideoxy-sequencing of the whole genes. The host *E. coli* strain THZ2 (Grauschopf *et al*., 1995) lacking the chromosomal *dsbA* gene was used for expression and phenotypic characterization of the mutant genes, where they are under control of the *trc* promotor and their expression is inducible by IPTG.

The *in vivo* activity of the *dsbA* mutants was tested by their ability to complement the dsbA$^-$ phenotype of *E. coli* THZ2 (Grauschopf *et al.*, 1995), which is immotile due to its inability to form disulfide bridges in the P-ring protein of the flagellar motor (Dailey & Berg, 1993). In addition, *E. coli* THZ2 harbors a gene encoding the MalF−β-galactosidase 102 fusion protein that only results in a Lac$^+$ phenotype when disulfide bond formation does not occur in the periplasm (Bardwell *et al*., 1991, 1993; Grauschopf *et al*., 1995). All *dsbA* mutants restored motility on soft agar and disulfide bond forming activity in the periplasm. Identical results were obtained on rich medium and on synthetic rich medium without any thiol and disulfide compounds. Therefore, disulfide compounds of the growth medium can almost certainly be excluded as periplasmic oxidants, and all the DsbA variants are likely to be reoxidized by DsbB with an efficiency similar to that of DsbA WT.

The DsbA variants were purified from periplasmic extracts as described previously (Hennecke *et al.*, 1997). The yields of the purified proteins were ≥20 mg of DsbA per liter of bacterial culture. All variants were oxidized to more than 99% after purification as judged by Ellman's assay (1959). All amino acid replacements were confirmed by electrospray mass spectrometry. The extinction coefficients of the variants were determined according to Gill and von Hippel (1989) and are summarized in Table 1.

The catalytic activities of the variants were quantified by their ability to accelerate the reduction of GSSG by reduced DTT at pH 4.5 (Wunderlich *et al.*, 1995) and were almost identical to the activity of DsbA WT (Table 1). Hence, W76, W126, and F26 do not sigificantly influence disulfide exchange reactions between DsbA and small organic thiols.

Circular Dichroism Spectra. The influence of the amino acid replacements on the secondary and tertiary structure of DsbA was analyzed by far- and near-UV circular dichroism spectra. The far-UV CD spectra of the oxidized and reduced variants are very similar to those of DsbA WT. Their shape is typical for proteins rich in α-helices, with a maximum around 191 nm and minima around 208 and 222 nm (Wunderlich *et al.*, 1993b; data not shown). Similar to DsbA WT, there are no major changes in the far-UV CD spectra upon reduction of the active-site disulfide bridge in any variant. In the case of the variants W76F, W126F, and W76F/W126F, a small decrease of the CD signal around 227 nm was observed. Since tryptophans usually also contribute to CD spectra in the far-UV range (Mulkerrin, 1996), it is likely that these changes result from the removal of the tryptophans rather than from structural changes in the protein.

Near-UV CD spectra reflect the asymmetric environment of aromatic amino acid side chains (mainly tryptophan) and disulfide bridges, which is indicative for a properly folded and compact tertiary structure. The oxidized form of DsbA WT has a negative band at 286 nm and a broad, slightly positive band around 305 nm (Figure 2A). The spectral changes upon reduction of DsbA lead to a loss of the band around 305 nm and a strong signal increase below 265 nm. These characteristic features were also observed for all variants, indicating their properly folded tertiary structure.

The difference spectra between the oxidized and reduced forms of DsbA WT and the variants are identical for all proteins with a small maximum around 300 nm and a strongly decreasing $\Delta\Theta$ value below 265 nm (Figure 2B). Therefore, changes in the tertiary structure which may occur upon reduction of the catalytic disulfide must be very similar in DsbA WT and the variants.

The contributions of the tryptophans to the near-UV CD spectra of oxidized and reduced DsbA were determined by calculating the difference spectra between DsbA WT and each single-tryptophan variant (Figure 2C). W76 shows a well-defined negative band at 292 nm and a broader positive band around 250 nm. In contrast, W126 shows three negative bands at 266, 287, and 294 nm and a strongly increasing signal below 260 nm. The contributions of both tryptophans to the near-UV CD spectra of DsbA are identical for the oxidized and reduced forms and are additive, as the sum of these single-tryptophan contributions is practically identical to the difference spectrum between DsbA WT and the W76F/W126F variant (Figure 2C).

Fluorescence Spectra and Quantum Yields of the DsbA Variants. Analysis of the fluorescence spectra of the variants W76F, W126F, W76F/W126F, and F26L revealed that the variant W76F does not exhibit any tryptophan fluorescence in its native, oxidized and native, reduced forms (Figure 3, Table 1). However, about half of the fluorescence of unfolded DsbA WT is restored after its denaturation by GdmCl (Figure 3, Table 1). Obviously, the fluorescence of W126 is fully quenched in native DsbA, and W76 is exclusively responsible for DsbA's fluorescence in the native state as well as the increase in fluorescence upon reduction of the active-site disulfide. Unexpectedly, the fluorescence of reduced W126F is even 1.5-fold higher than that of reduced WT, with a 4.6-fold fluorescence increase compared to oxidized W126F. This observation can possibly be explained by a unidirectional, nonradiative energy transfer from W76 to W126 and the presence of a static quenching component in oxidized W126F (see below).

In the three-dimensional structure of oxidized DsbA WT, F26 from the thioredoxin domain makes an interdomain

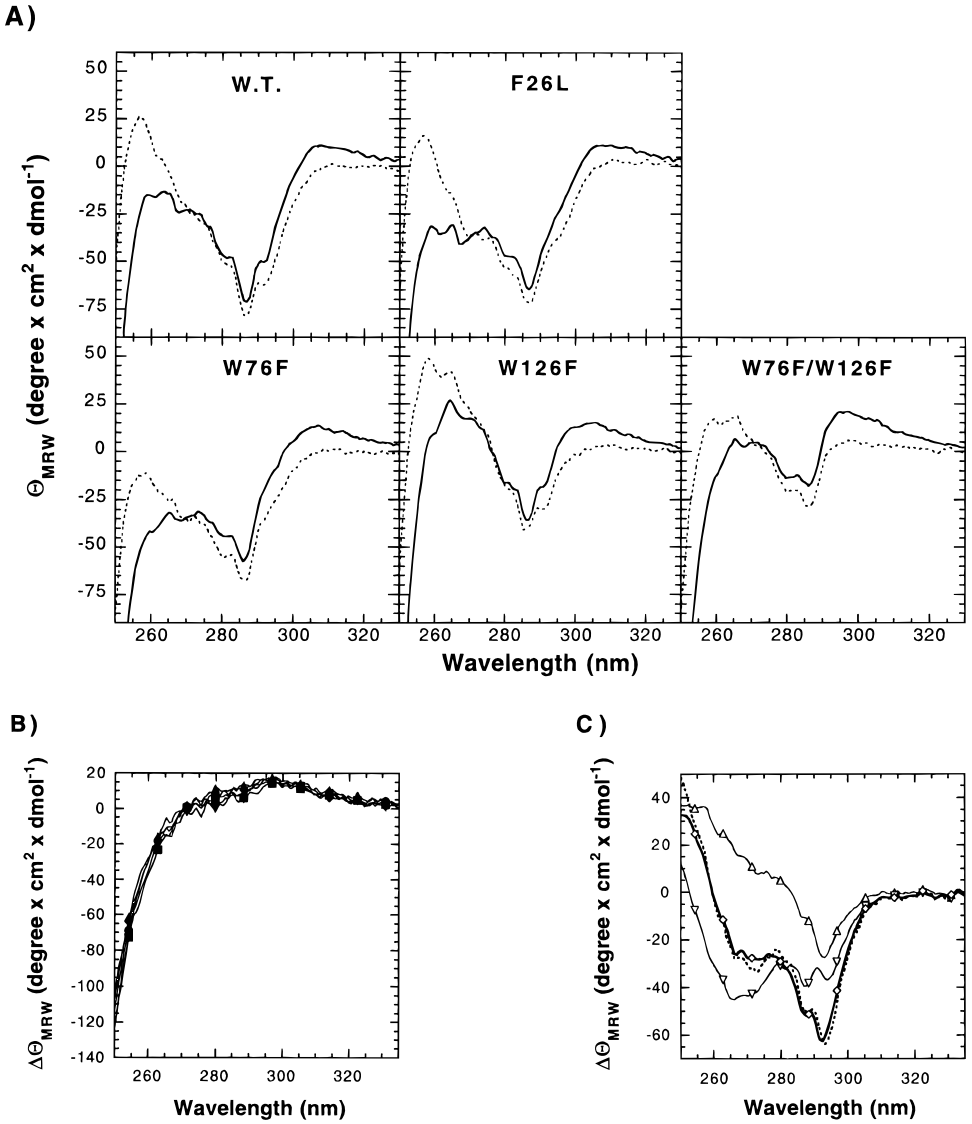

FIGURE 2: Near-UV circular dichroism spectra of DsbA WT and its variants. (A) Spectra of oxidized (solid line) and reduced (dashed line) DsbA were recorded at 25 °C in 10 mM sodium sulfate, 1 mM sodium phosphate, pH 7.0. (B) Difference spectra between oxidized and reduced DsbA WT (●), F26L (■), W76F (▲), W126F (▼), and W76F/W126F (◆), reflecting the contribution of the disulfide bridge. (C) Contributions of tryptophans as determined from the difference spectra WT−W76F (△), WT−W126F (▽), and WT−W76F/W126F (◇). The dotted line represents the sum of the contributions of the single tryptophans [(WT−W76F) + (WT−W126F)]. Only the difference spectra for the reduced proteins are shown.

contact with W76 and is also close to the sulfur of C33. F26 is thus a good candidate for being involved in the disulfide-induced quenching of DsbA's fluorescence. Indeed, a 2-fold fluorescence increase is observed for the oxidized F26L variant compared to DsbA WT, whereas the fluorescence of reduced F26L is practically identical to that of reduced WT (Figure 3, Table 3). The fluorescence of the F26L variant thus increases only about 1.7-fold upon reduction (Table 3).

Time-Resolved Fluorescence Parameters. Fluorescence lifetime measurements of oxidized and reduced DsbA and its variants were performed at pH 7.0 and at emission wavelengths ranging from 340 to 360 nm in 10 nm intervals. Single and double exponential fits of the data yielded unacceptable high values of χ_R^2. The best results with a χ_R^2 close to 1 and no systematic deviations in the autocorrelation function of the residuals were obtained with a triple exponential fit (Figure 4). In order to improve the recovery of the decay parameters, a *global analysis* of all phase measurements at the different wavelengths was performed (Beechem *et al.*, 1983). The results of the lifetime analysis for DsbA WT and its variants are shown in Table 2.

Table 3 shows the relative changes of the quantum yields, the fluorescence intensities (at 340 nm), and the amplitude-weighted average lifetimes accompanying disulfide bond reduction or amino acid replacement. Since the changes of the fluorescence intensities and of the amplitude-weighted average lifetimes are very similar, the quenching processes are of purely dynamic nature (see eqs 1 and 2). Only the variant W126F is an exception and shows a considerable static quenching component.

Solvent Accessibility of the Tryptophans. The solvent-accessible surface area of W76 and W126 in the crystal structure of oxidized DsbA (Martin *et al.*, 1993) is 7 and 45 Å^2, respectively, as calculated with the program DSSP (Kabsch & Sander, 1983). We analyzed the redox state-dependent accessibility of W76 and W126 by measuring their dynamic quenching by acrylamide. Interestingly, acrylamide-induced quenching of tryptophan fluorescence is slightly higher for reduced DsbA compared to the oxidized

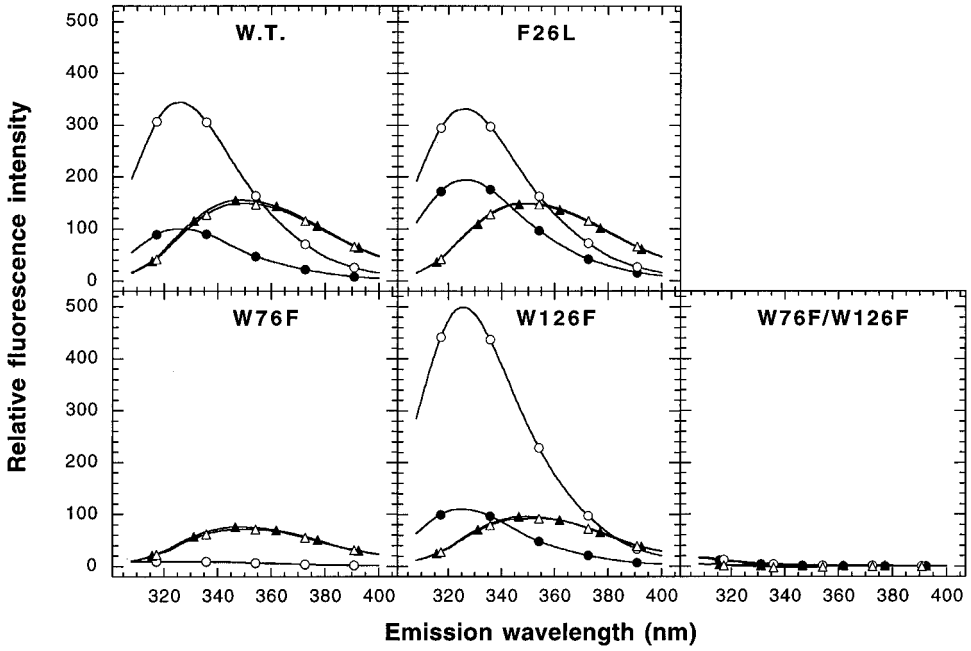

FIGURE 3: Fluorescence emission spectra of DsbA WT and its variants. Spectra of native oxidized (●), native reduced (○), unfolded oxidized (▲), and unfolded reduced (△) proteins were recorded at 25 °C in 100 mM sodium phosphate, pH 7.0 (excitation at 295 nm). The fluorescence maximum of oxidized WT was arbitrarily set to 100 fluorescence units.

Table 2: Calculated Lifetimes (τ), Amplitude Fractions (a), and Amplitude-Weighted Average Lifetimes ($\langle\tau\alpha\rangle$) at 340 nm, and χ_R^2 As Obtained by Global Analysis of the Fluorescence Decay of DsbA and Its Variants F26L and W126F at pH 7.0 in the Oxidized and Reduced States

	a_1	τ_1 (ns)	a_2	τ_2 (ns)	a_3	τ_3 (ns)	χ_R^2	$\langle\tau\alpha\rangle$ (ns)
WT_{ox}	0.286 ± 0.011	0.143 ± 0.021	0.672 ± 0.020	1.003 ± 0.028	0.042 ± 0.023	3.038 ± 0.172	2.2	0.84
WT_{red}	0.188 ± 0.028	0.134 ± 0.029	0.149 ± 0.009	2.778 ± 0.087	0.664 ± 0.029	3.632 ± 0.103	0.9	2.85
$F26L_{ox}$	0.252 ± 0.015	0.335 ± 0.058	0.711 ± 0.024	2.032 ± 0.082	0.036 ± 0.028	4.504 ± 1.108	2.4	1.69
$F26L_{red}$	0.208 ± 0.013	0.159 ± 0.015	0.282 ± 0.019	2.169 ± 0.061	0.511 ± 0.014	3.435 ± 0.087	1.4	2.40
$W126F_{ox}$	0.141 ± 0.003	0.383 ± 0.039	0.765 ± 0.025	1.262 ± 0.092	0.094 ± 0.025	3.097 ± 0.370	1.3	1.31
$W126F_{red}$	0.014 ± 0.022	0.447 ± 0.059	0.377 ± 0.015	1.904 ± 0.127	0.608 ± 0.016	4.904 ± 0.019	0.8	3.70

protein (Figure 5). As W76 is mainly responsible for the fluorescence in DsbA, the increased acrylamide quenching in reduced DsbA can be assigned to this tryptophan. In contrast, the extremely low tryptophan fluorescence of the variant W76F is quenched to the same degree in the oxidized and reduced form. Interestingly, the fluorescence of oxidized F26L is already quenched by acrylamide as effective as in the reduced form, which might reflect its strongly decreased thermodynamic stability (see below).

Reversible Folding/Unfolding and Redox Properties of the Variants. Since W76 and F26 form an important interdomain contact in the structure of oxidized DsbA, the thermodynamic stabilities of the variants W76F and F26L were determined by GdmCl-induced unfolding/refolding transitions (Figure 6, Table 5) which were followed fluorometrically. Similar to DsbA WT, the transitions of the variants F26L and W76F are fully reversible, and their reduced forms are more stable than their oxidized forms. Compared to reduced DsbA WT, reduced F26L and W76F are destabilized by 14.8 and 18.2 kJ/mol, respectively, and the cooperativities of the transitions are similar to the cooperativity of reduced DsbA WT. In contrast, the oxidized forms of F26L and W76F exhibit strongly decreased cooperativities of folding. Compared to the *m*-value of 25.5 kJ/(mol·M) of oxidized DsbA WT, the cooperativities are reduced to 5.9 kJ/(mol·M) and 12.9 kJ/(mol·M), respectively. It is therefore uncertain whether the oxidized forms of the variants still fold according to the two-state model. In principle, the stronger destabilization of the oxidized forms of F26L and W76F compared to their reduced forms should lead to a more oxidizing redox potential compared to DsbA WT.

The redox potentials of the variants F26L and W126F were determined by measuring their equilibrium constants (K_{eq}) with glutathione (Wunderlich & Glockshuber, 1993). With a K_{eq} of 0.13 mM at pH 7.0, the DsbA WT protein is the most oxidizing member of the thiol−disulfide oxidoreductase family (Wunderlich & Glockshuber, 1993). While the redox potential of W126F is unchanged compared to DsbA WT, the variant F26L is 14 mV more oxidizing than the WT (Table 5), which is consistent with its strongly destabilized oxidized form.

DISCUSSION

Reduction of the active-site disulfide in thioredoxin and DsbA causes a strong increase in tryptophan fluorescence (Holmgren, 1972; Wunderlich & Glockshuber, 1993; Zapun *et al.*, 1993). However, the tryptophan fluorophores are located at completely different positions in the primary and tertiary structure of these enzymes. While fluorescence quenching in thioredoxin is static and caused by a direct contact between the disulfide and W28 (Mérola *et al.*, 1989), the two tryptophans in DsbA, W76 and W126, are not located in the thioredoxin-like domain and are about 12 and 20 Å away from the active-site disulfide, respectively. We studied

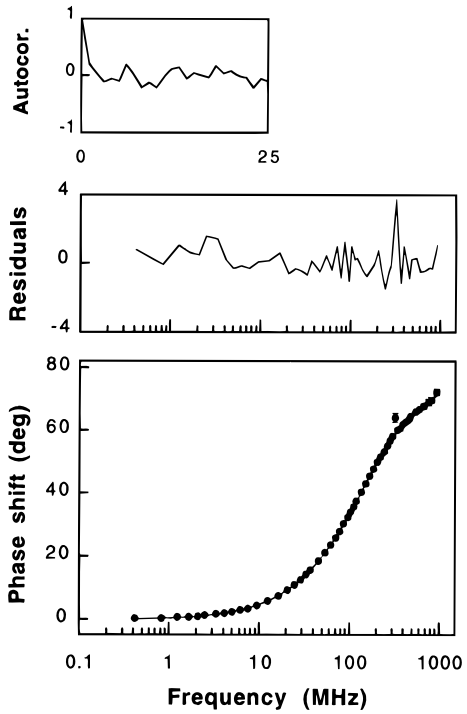

FIGURE 4: Multifrequency phase fluorometric data of oxidized DsbA WT and graphical tests used for data analysis. Measured phase angles are plotted versus frequency and fitted for a sum of three exponentials (bottom). Also included are plots of the weighted residuals (middle) and of their autocorrelation function (top) as a function of frequency.

Table 3: Redox State-Dependent Changes in the Tryptophan Fluorescence

	Q'/Q[a]	I'/I[b]	$\langle\tau\alpha\rangle'/\langle\tau\alpha\rangle$[c]
$WT_{ox} \rightarrow WT_{red}$	3.30	3.30	3.39
$F26L_{ox} \rightarrow F26L_{red}$	1.46	1.70	1.42
$WT_{ox} \rightarrow F26L_{ox}$	1.93	2.10	2.01
$WT_{red} \rightarrow F26L_{red}$	0.91	0.93	0.84
$W126F_{ox} \rightarrow W126F_{red}$	4.40	4.56	2.80

[a] Q: relative increase in quantum yield. [b] I: relative increase in fluorescence intensity at 340 nm (excitation at 295 nm). [c] $\langle\tau\alpha\rangle$: relative increase in amplitude-weighted average lifetime at 340 nm.

DsbA's fluorescence properties by replacing the tryptophans by phenylalanines in a set of variants (W76F, W126F, and W76F/W126F).

The W76F replacement almost completely extinguishes the fluorescence of both the oxidized and reduced forms of DsbA and thus identifies W76 as the only active tryptophan fluorophore in DsbA. W76 is buried in the hydrophobic domain interface of the protein. Consistently, the fluorescence emission maximum of DsbA WT (326 nm) is blue-shifted compared to that of *E. coli* thioredoxin (341 nm), where the important fluorophore W28 is significantly solvent-exposed (Katti *et al.*, 1990; Jeng *et al.*, 1994).

Surprisingly, the fluorescence of W126 is fully quenched in both redox states of DsbA. The reason for this quenching is not obvious. However, the side chains of Q74 and/or N127 might be responsible for this effect, since amide groups have been reported as quenchers of tryptophan fluorescence (Bushueva *et al.*, 1975).

Despite the removal of a potential fluorophore, the reduced variant W126F shows a 1.5-fold higher fluorescence compared to reduced DsbA WT. A comparable observation was made for *E. coli* thioredoxin (Krause & Holmgren, 1991; Slaby *et al.*, 1996) and barnase (Loewenthal *et al.*, 1991; Willaert *et al.*, 1992) upon removal of one of the tryptophans. In case of DsbA, this phenomenon can be explained by the lack of energy transfer from W76 to W126 in the variant W126F and the lack of static quenching in the reduced W126F variant.

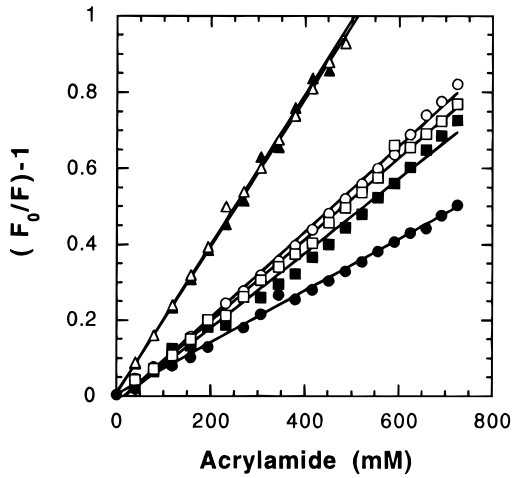

FIGURE 5: Acrylamide-induced quenching of tryptophan fluorescence of DsbA WT (●, ○) and its variants W76F (▲, △) and F26L (■, □) in their oxidized (closed symbols) and reduced (open symbols) forms. The protein concentration was 10 μM in 80 mM sodium phosphate, pH 7.0. A Stern−Volmer plot is shown. F_0 corresponds to the fluorescence in the absence of acrylamide, and F is the measured fluorescence.

Table 4: Rate Constants of Fluorescence Decay (k), Apparent Rate Constants of Energy Transfer (k_{Etr}), and Dynamic Quenching (k_Q) Derived from the Lifetimes with the Largest Amplitude

	k[a] (ns^{-1})	k_{Etr} (ns^{-1})	k_Q[b] (ns^{-1})
WT_{ox}	1.00	0.21	0.59
WT_{red}	0.27	0.07	
$F26L_{ox}$	0.49	0.21	0.08
$F26L_{red}$	0.29	0.09[c]	
$W126F_{ox}$	0.79		0.59
$W126F_{red}$	0.20[d]		

[a] $k = 1/\tau = 0.20\ ns^{-1} + k_{Etr} + k_Q$, using τ of major amplitude. [b] Dynamic quenching is assumed to occur exclusively in the oxidized state, k_Q. [c] Could also contain a contribution from a conformational effect of the replacement F26L on W76. [d] This rate constant is assumed to be the intrinsic rate constant of fluorescence decay (k_{intr}) of W76.

Disulfides are known to be effective quenchers of tryptophan fluorescence (Cowgill, 1967). However, in the case of DsbA the question arises how the disulfide is able to quench the fluorescence of W76 although it is more than 12 Å away. Since F26 makes a van der Waals contact with both W76 and C33 of the catalytic disulfide, we assumed that it is involved in the quenching process. Indeed, exchange of the aromatic residue F26 against leucine diminishes disulfide-dependent quenching of W76, while the steady-state fluorescence properties of the reduced F26L variant remain essentially unchanged. As the fluorescence of oxidized F26L is still 1.7-fold lower than that of the reduced variant, a limited, redox-state-dependent quenching of W76 still occurs in F26L.

We can conclude from the fluorescence intensity and lifetime measurements that two distinct quenching processes can be operative: unidirectional nonradiative energy transfer from W76 to W126, and dynamic quenching by the disulfide bond or the −SH groups.

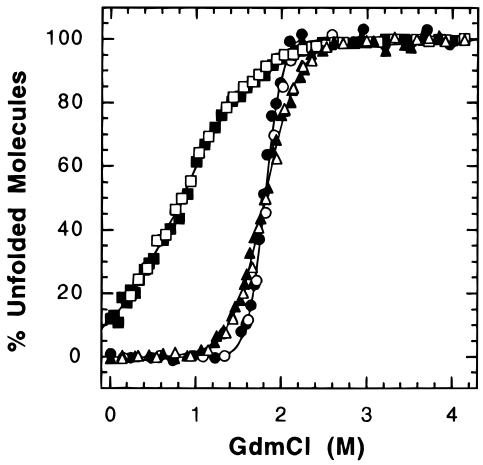

FIGURE 6: Reversible, GdmCl-dependent unfolding/refolding transitions of oxidized DsbA WT (●, ○) and its variants W76F (▲, △) and F26L (■, □) at pH 7.0 and 25 °C. Unfolding and refolding experiments are represented by closed symbols and open symbols, respectively. The fraction of unfolded molecules at equilibrium was calculated from the original data by a six-parameter fit according to the two-state model (Santoro & Bolen, 1988).

Different lifetimes for a single tryptophan are usually explained in terms of the existence of different conformers of that residue (Szabo & Rayner, 1980). We focused our analysis on the lifetime component with the highest amplitude fraction, which should represent the most populated conformer. Qualitatively, the same results were obtained with the amplitude-weighted average lifetime. The simplest situation is found in the reduced variant W126F, where no energy transfer from W76 to W126 and no quenching by the disulfide bridge occur. Since the lifetime of W76 is relatively long (5 ns), the possible quenching by the −SH groups must be very small. We therefore made the simplifying assumption that the lifetime of W76 in the reduced variant W126F equals the intrinsic lifetime of W76 in all oxidized and reduced DsbA proteins.

In the variant W126F, the decreased fluorescence of W76 in the oxidized protein is exclusively caused by quenching by the disulfide. The dynamic part of quenching can be described by eq 5:

$$1/\tau = 1/\tau_{intr} + k_Q \qquad (5)$$

where τ_{intr} is the lifetime in the absence of quenching and k_Q is the rate constant of quenching. If we assume that the conformational effects of oxidation on the intrinsic lifetimes are negligible, we can use τ_{intr} from the reduced variant W126F and estimate k_Q. Applying this to the variant W126F gives a k_Q of 0.59 ns^{-1} (Table 4).

The differences between the lifetimes of the reduced variants W126F and F26L can only be due to nonradiative energy transfer from W76 to W126 as described by eq 6:

$$1/\tau = 1/\tau_{intr} + k_{Etr} \qquad (6)$$

where τ_{intr} is the lifetime in the absence of energy transfer and k_{Etr} is the apparent rate constant of energy transfer (in principle, k_{Etr} may also contain contributions caused by conformational changes resulting from the replacement W126F). Using the data of Table 4, we calculated $k_{Etr} = 0.09$ ns^{-1} for the reduced F26L variant. Applying the same consideration to the reduced WT and W126F variant gives a similar value for k_{Etr} of 0.07 ns^{-1} (Table 4).

Since the difference between the fluorescence of oxidized WT and the oxidized W126 variant can only be due to the energy transfer from W76 to W126, we calculated an energy transfer rate constant for oxidized WT of $k_{Etr} = 0.21$ ns^{-1}. The nonradiative energy transfer is thus more efficient in the oxidized state than in the reduced state, possibly due to a different orientation of W76 relative to W126.

If the orientations of W76 in the oxidized and reduced F26L variant are the same as in oxidized and reduced DsbA WT, the energy transfer to W126 ($k_{Etr} = 0.21$ ns^{-1}) should also be increased in the oxidized variant F26L, and a k_Q of 0.08 ns^{-1} can be calculated for the quenching by the disulfide bridge in the F26L protein. The quenching efficiency is thus strongly reduced in the absence of F26 (Table 4).

The overall conclusion is that energy transfer from W76 to W126 appears in both redox states, but is more pronounced in the oxidized state. Only the disulfide bridge is able to create a dynamic quenching of W76, and it largely needs F26 for this effect. The overall situation of dynamic quenching and energy transfer processes in oxidized and reduced DsbA WT can therefore be represented by Scheme 1.

Since $k_{intr} = 0.20$ ns^{-1} can be considered as a lower limit, the rate constants for k_Q and k_{Etr} are upper limits. Only in

Table 5: Redox Properties and Thermodynamic Stabilities of DsbA WT and DsbA Variants at 25 °C and pH 7.0

	K_{eq} (mM)[a]	$E'_{0,DsbA}$ (V)[b]	transiton midpoint (M GdmCl)[c]	cooperativity [kJ/(mol·M) GdmCl][c]	ΔG_{stab} (kJ/mol)[c]	$\Delta\Delta G_{ox/red}$ (kJ/mol)[d]
WT	0.131 ± 0.004	−0.125				12.4 ± 5.5
oxidized			1.80	25.5 ± 1.6	−46.0 ± 2.9	
reduced			2.37	24.6 ± 1.1	−58.4 ± 2.6	
F26L	0.043 ± 0.002	−0.111				(38.3 ± 3.2)
oxidized			0.90	(5.9 ± 0.3)	(−5.3 ± 0.9)	
reduced			1.89	23.1 ± 1.2	−43.6 ± 2.3	
W76F	nd	nd				(17.0 ± 3.0)
oxidized			1.80	(12.9 ± 0.4)	(−23.2 ± 0.8)	
reduced			1.90	21.2 ± 1.2	−40.2 ± 2.2	
W126F	0.119 ± 0.001	−0.124				nd
oxidized			nd	nd	nd	
reduced			nd	nd	nd	

[a] Equilibrium constant with GSH/GSSG. Refer to the Experimental Procedures for details. [b] The redox potential of DsbA was calculated using an E'_0 of −0.240 V for GSH/GSSG. [c] Data were evaluated according to the two-state model of folding. The two-state model is probably not valid for the oxidized forms of variants F26L and W76F, since the cooperativities of their transitions (*m*-values) are strongly reduced. [d] $\Delta\Delta G_{ox/red}$: difference between the free energies of folding of oxidized and reduced DsbA. A possible influence of the disulfide bond on the entropy of unfolded oxidized DsbA was not considered.

Scheme 1

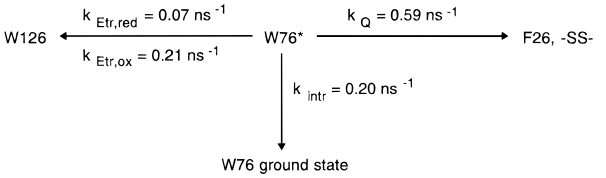

the oxidized variant W126F was a static component of the disulfide-dependent quenching of W76 observed. It is not clear why such a static component is not apparent in the oxidized WT.

From the known 2.0 Å X-ray structure of oxidized DsbA, a value of 0.122 is calculated for the efficiency of energy transfer (E) from W76 to W126 in the oxidized WT ($J_{AD} = 1.64 \times 10^{-16}$ cm^6 mmol^{-1}, $\phi_D = 4.49 \times 10^{-2}$, $n = 1.5$, $\kappa^2 = 0.709$, $R_0 = 9.84$ Å, $R = 13.66$ Å). The efficiency of energy transfer was also calculated from experimental rate constants according to eq 3 and yields values of 0.31 and 0.43 in the reduced and oxidized variant F26L and 0.26 and 0.21 in the reduced and oxidized WT, respectively. These values are about 3-fold higher than theoretically expected. This can principally result from an overestimation of k_{Etr} due to conformational changes caused by the mutations, from an overestimation of the average distance between W76 and W126 in the solution structure of DsbA, and from the error in the calculation of J_{AD}.

We also used the variants W76F, W126F, and W76F/W126F to determine the contribution of tryptophan residues to the circular dichroism spectra of DsbA. The structurally conservative replacement of tryptophan by phenylalanine has only minor effects on the far-UV CD spectra, whereas the near-UV CD spectra differ strongly compared to the WT protein. Bands in the near-UV CD arising from tryptophans are generally dominating and much stronger than bands caused by phenylalanines (Strickland, 1974). The changes in the near-UV CD spectra of the above DsbA variants should thus yield the contributions of the single tryptophan residues. We did not expect altered near-UV CD spectra due to conformational changes, since the far-UV CD spectra are almost identical for DsbA WT and all variants. We found that the net contributions of W76 and W126 to the near-UV CD spectra were additive and of opposite ellipticity in the range of 285−250 nm. The additive effect of both tryptophans was expected, since they are not in direct contact in the structure of DsbA. Similar observations have been made for other proteins (Vuilleumier *et al.*, 1993).

Data on the contribution of protein disulfides to near-UV CD spectra of proteins are rare (Mulkerrin, 1996), as their reduction often leads to large conformational changes or complete unfolding of the protein. In DsbA, reduction of the disulfide causes changes in the near-UV CD spectra that reflect either the contribution of the disulfide itself and/or accompanying conformational changes. The difference spectra (Figure 2B) show that the disulfide makes a strong contribution of negative ellipticity to the near-UV CD of DsbA in the range of 270−250 nm and a broad, positive band around 295 nm.

The contact between F26 and W76 represents an important part of the interactions between the thioredoxin domain and the α-helical domain of oxidized DsbA (Martin *et al*., 1993). F26 is strictly conserved among all currently known DsbA sequences and is located at the same position in the primary and tertiary structure as W28 in thioredoxin. Despite the conservation of F26, the replacement F26L does not influence the catalytic activity of DsbA *in vivo*. However, it makes the redox potential of DsbA 14 mV more oxidizing. The F26L variant of DsbA is indeed the most oxidizing disulfide oxidoreductase reported so far. The exchanges of F26L and W76F have a strong effect on the GdmCl-induced unfolding transitions of oxidized DsbA. The cooperativities of the transitions of the oxidized forms of the variants F26L and W76F are strongly decreased, indicating that these variants no longer fold according to a two-state process (Pace, 1986; Myers *et al.*, 1995). The reduced forms of F26L and W76F are also destabilized compared to reduced DsbA WT, but unfold/refold with cooperativities similar to the cooperativity of reduced DsbA WT. Both the oxidized and reduced forms of the variants F26L and W76F are less stable than the corresponding forms of DsbA WT, which reflects the importance of the F26/W76 interdomain contact. In addition, the increased susceptibility of W76 to acrylamide quenching in the oxidized variant F26L relative to oxidized DsbA WT (Figure 5) confirms the importance of the interaction between W76 and F26 for the stability of oxidized DsbA WT. The redox-state-dependent quenching of W76 by acrylamide in DsbA WT is also the only direct evidence that at least small confirmational changes occur upon reduction of the enzyme. Overall, the main reason for the strict conservation of F26 appears to be the stabilization of DsbA's oxidized form.

In conclusion, we have shown that only one tryptophan, W76, is responsible for the fluorescence increase occurring upon reduction of the active-site disulfide of DsbA. In oxidized DsbA, the fluorescence of W76 is diminished by an intramolecular, dynamic quenching mechanism, involving contacts with F26 and the disulfide, and by energy transfer to W126. In the reduced WT, only the energy transfer to W126 remains as the major quenching mechanism. In the variant W126F, there is also a static component in the disulfide-induced quenching of W76. Knowledge of the three-dimensional structure of reduced DsbA will be required to decide whether these different quenching mechanisms are accompanied by redox state-dependent conformational changes.

ACKNOWLEDGMENT

We thank A. Jacobi for fruitful discussions, V. Eggli for help during construction of the DsbA mutants, and P. James for performing electrospray mass spectrometry.

REFERENCES

Bardwell, J. C. A., & Beckwith, J. (1993) *Cell 74*, 769−771.
Bardwell, J. C. A., McGovern, K., & Beckwith, J. (1991) *Cell 67*, 581−589.
Bardwell, J. C. A., Lee, J.-O., Jander, G., Martin, N., Belin, D., & Beckwith, J. (1993) *Proc. Natl. Acad. Sci. U.S.A. 90*, 1038−1042.
Beechem, J. M., Knutson, J. R., Ross, J. B. A., Turner, B. W., & Brand, L. (1983) *Biochemistry 22*, 6054−6058.
Bushueva, T. L., Busel, E. P., & Burstein, E. A. (1975) *Stud. Biophys. 52*, 41−52.
Chen, R. F. (1967) *Anal. Lett. 1*, 35−42.
Cowgill, R. W. (1967) *Biochim. Biophys. Acta 140*, 37−44.
Dailey, F. E., & Berg, H. C. (1993) *Proc. Natl. Acad. Sci. U.S.A. 90*, 1043−1047.
Darby, N. J., & Creighton, T. E. (1995) *Biochemistry 34*, 3576−3587.
Desie, G., Boens, N., & De Schryver, F. C. (1986) *Biochemistry 25*, 8301−8308.

Eftink, M. R., & Ghiron, C. A. (1976) *J. Phys. Chem. 80*, 486−493.
Ellman, G. L. (1959) *Arch. Biochem. Biophys. 82*, 70−77.
Förster, T. (1948) *Ann. Phys.* (*Leipzig) 2*, 55−75.
Gilbert, H. F. (1990) *Adv. Enzymol. Relat. Areas Mol. Biol. 63*, 69−172.
Gill, S. C., & von Hippel, P. H. (1989) *Anal. Biochem. 182*, 319−326.
Grauschopf, U., Winther, J. R., Korber, P., Zander, T., Dallinger, P., & Bardwell, J. C. A. (1995) *Cell 83*, 947−955.
Griffey, R. H., & Redfield, A. G. (1985) *Biochemistry 24*, 817−822.
Guilhot, C., Jander, G., Martin, N. L., & Beckwith, J. (1995) *Proc. Natl. Acad. Sci. U.S.A. 92*, 9895−9899.
Harris, D. L., & Hudson, B. S. (1990) *Biochemistry 29*, 5276−5285.
Hennecke, J., Spleiss, C., & Glockshuber, R. (1997) *J. Biol. Chem. 272*, 189−195.
Holmgren, A. (1972) *J. Biol. Chem. 247*, 1992−1998.
Jander, G., Martin, N. L., & Beckwith, J. (1994) *EMBO J. 13*, 5121−5127.
Jeng, M.-F., Campbell, A. P., Begley, T., Holmgren, A., Case, D. A., Wright, P. E., & Dyson, H. J. (1994) *Structure 2*, 853−868.
Kabsch, W., & Sander, C. (1983) *Biopolymers 22*, 2577−2637.
Kamitani, S., Akiyama, Y., & Ito, K. (1992) *EMBO J. 11*, 57−62.
Katti, S. K., LeMaster, D. M., & Eklund, H. (1990) *J. Mol. Biol. 212*, 167−184.
Kishigami, S., Kanaya, E., Kikuchi, M., & Ito, K. (1995) *J. Biol. Chem. 270*, 17072−17074.
Kraulis, P. J. (1991) *J. Appl. Crystallogr. 24*, 946−950.
Krause, G., & Holmgren, A. (1991) *J. Biol. Chem. 266*, 4056−4066.
Kunkel, T. A. (1985) *Proc. Natl. Acad. Sci. U.S.A. 82*, 488−492.
Kunkel, T. A., Roberts, J. D., & Zakour, R. A. (1987) *Methods Enzymol. 154*, 367−382.
Loewenthal, R., Sancho, J., & Fersht, A. R. (1991) *Biochemistry 30*, 6775−6779.
Loferer, H., & Hennecke, H. (1994) *Trends Biochem. Sci. 19*, 169−171.
Loferer, H., Bott, M., & Hennecke, H. (1993) *EMBO J. 12*, 3373−3383.
Loferer, H., Wunderlich, M., Hennecke, H., & Glockshuber, R. (1995) *J. Biol. Chem. 270*, 26178−26183.
Martin, J. L. (1995) *Structure 3*, 245−250.
Martin, J. L., Bardwell, J. C. A., & Kuriyan, J. (1993) *Nature 365*, 464−468.
Mérola, F., Rigler, R., Holmgren, A., & Brochon, J.-C. (1989) *Biochemistry 28*, 3383−3398.
More, J. J., & Sorensen, D. C. (1983) *SIAM J. Sci. Stat. Comput. 4*, 553−572.
Mulkerrin, M. G. (1996) *Spectroscopic methods for determining protein structure in solution*, pp 5−27, VCH Publishers, New York.
Myers, J. K., Pace, C. N., & Scholtz, J. M. (1995) *Protein Sci. 4*, 2138−2148.
Pace, C. N. (1986) *Methods Enzymol. 131*, 266−280.
Parker, C. A., & Rees, W. T. (1960) *Analyst 85*, 587−600.
Rost, J., & Rapoport, S. (1964) *Nature 201*, 185.
Santoro, M. M., & Bolen, D. W. (1988) *Biochemistry 27*, 8063−8068.
Sillen, A., Vos, R., & Engelborghs, Y. (1996) *Photochem. Photobiol. 64*, 785−791.
Slaby, I., Cerna, V., Jeng, M.-F., Dyson, H. J., & Holmgren, A. (1996) *J. Biol. Chem. 271*, 3091−3096.
Strickland, E. H. (1974) *CRC Crit. Rev. Biochem. 3*, 113−175.
Szabo, A. G. (1989) in *The Enzyme Catalysis Process* (Cooper, A., Houben, J., & Chein, L. C., Eds.) pp 123−139, Plenum Press, New York.
Szabo, A. G., & Rayner, D. M. (1980) *J. Am. Chem. Soc. 102*, 554−563.
Vieira, J., & Messing, J. (1987) *Methods Enzymol. 153*, 3−11.
Vuilleumier, S., Sancho, J., Loewenthal, R., & Fersht, A. R. (1993) *Biochemistry 32*, 10303−10313.
Weber, G. (1981) *J. Phys. Chem. 85*, 949−953.
Willaert, K., Loewenthal, R., Sancho, J., Froeyen, M., Fersht, A., & Engelborghs, Y. (1992) *Biochemistry 31*, 711−716.
Wunderlich, M., & Glockshuber, R. (1993) *Protein Sci. 2*, 717−726.
Wunderlich, M., Otto, A., Seckler, R., & Glockshuber, R. (1993a) *Biochemistry 32*, 12251−12256.
Wunderlich, M., Jaenicke, R., & Glockshuber, R. (1993b) *J. Mol. Biol. 233*, 559−566.
Wunderlich, M., Otto, A., Maskos, K., Mücke, M., Seckler, R., & Glockshuber, R. (1995) *J. Mol. Biol. 247*, 28−33.
Yamamoto, Y., & Tanaka, J. (1972) *Bull. Chem. Soc. Jpn. 45*, 1362−1366.
Zapun, A., & Creighton, T. E. (1994) *Biochemistry 33*, 5202−5211
Zapun, A., Bardwell, J. C. A., & Creighton, T. E. (1993) *Biochemistry 32*, 5083−5092.

BI963017W